

## Longitudinal and transverse velocity fields in parsec-scale jets

---

Florent Mertens<sup>\*1</sup> and Andrei Lobanov<sup>1,2</sup>

<sup>1</sup>*Max-Planck-Institut für Radioastronomie*

*Auf dem Hugel 69, 53121 Bonn, Germany*

<sup>2</sup>*Institut für Experimentalphysik, Universität Hamburg*

*Luruper Chaussee 149, 22761 Hamburg, Germany*

*E-mail: [fmertens@mpifr.de](mailto:fmertens@mpifr.de), [alobanov@mpifr.de](mailto:alobanov@mpifr.de)*

Radio-loud AGN typically manifest powerful relativistic jets extending up to millions of light years and often showing superluminal motions organised in a complex kinematic pattern. A number of physical models are still competing to explain the jet structure and kinematics revealed by radio images using the VLBI technique. Robust measurements of longitudinal and transverse velocity field in the jets would provide crucial information for these models. This is a difficult task, particularly for transversely resolved jets in objects like 3C 273 and M 87. To address this task, we have developed a new technique for identifying significant structural patterns (SSP) of smooth, transversely resolved flows and obtaining a velocity field from cross-correlation of these regions in multi-epoch observations. Detection of individual SSP is performed using the wavelet decomposition and multiscale segmentation of the observed structure. The cross-correlation algorithm combines structural information on different scales of the wavelet decomposition, providing a robust and reliable identification of related SSP in multi-epoch images. The algorithm enables recovering structural evolution on scales down to 0.25 full width at half maximum (FWHM) of the image point spread function (PSF). We present here examples of applying this algorithm to obtain the first detailed transverse velocity fields and to study the kinematic evolution in the parsec-scale jets in 3C 273 and M 87.

*12th European VLBI Network Symposium and Users Meeting,  
7-10 October 2014  
Cagliari, Italy*

---

<sup>\*</sup>Speaker.

## 1. Introduction

The steady improvements of dynamic range of astronomical images and increasing complexity and detail of astrophysical modeling bring a higher demand on automatic (or *unsupervised*) methods for characterization and analysis of structural patterns in astronomical images.

A number of approaches developed in the fields of computer vision and remote sensing for tracking structural changes [*cf.*, 1] typically require *oversampling* in the temporal domain. This renders them difficult to be used in astronomical applications that requires tracking changes monitored with sparse sampling and dealing with partially transparent, *optically thin* structures.

Presently, structural decomposition of astronomical images normally involves simplified *supervised* techniques based on identification of specific features of the structure [2] or fitting the observed structure with a set of predefined templates (*e.g.*, two-dimensional Gaussian features).

A more robust approach to automatize identification and tracking of structural patterns in astronomical images can be provided by a generic multiscale method such as wavelet deconvolution or wavelet decomposition [*cf.*, 4]. In [5], we explored this wavelet approach and present a wavelet-based image segmentation and evaluation (WISE) method for structure decomposition and tracking in astronomical images. In this contribution, we present an overview of this new method along with results obtain on WISE analysis of parsec-scale radio jets in 3C 273 and 3C 120 compared with results of conventional structure analysis previously applied to these data. Finally, preliminary results of the velocity field analysis of the jet in M 87 is presented.

## 2. Wavelet-based Image Segmentation and Evaluation

To characterize the structure and structural evolution of an astronomical object, the imaged object structure needs to be decomposed into a set of significant structural patterns (SSP) that can be successfully tracked across a sequence of images. The multiscale decomposition provided by the wavelet transform [6] makes wavelets exceptionally well-suited to perform such a decomposition, yielding an accurate assessment of the noise variation across the image and warranting a robust representation of the characteristic structural patterns of the image. To adapt better to the needs of astronomical imaging, we have extended the multiscale approach to object detection, similarly to the methodology developed for the multiscale vision model [MVM; 4]. The method employs segmented wavelet decomposition (SWD) of individual images into arbitrary two-dimensional SSP (or image regions) and subsequent multiscale cross-correlation (MCC) of the resulting sets of SSP.

### 2.1 Segmented Wavelet Decomposition

The segmented wavelet decomposition (SWD) comprises the following steps to describe an image structure by a set of statistically significant patterns:

1. A wavelet transform is performed on an image  $I$  by decomposing the image into a set of  $J$  sub-bands (scales),  $w_j$ , and estimating the residual image noise (variable across the image).
2. At each sub-band, statistically significant wavelet coefficients are extracted from the decomposition by thresholding them against the image noise.

3. The significant coefficients are examined for local maxima, and a subset of the local maxima satisfying detection criteria is identified, defining the locations of SSP in the image.
4. Two-dimensional boundaries of the SSP are defined by the watershed segmentation using the feature locations as initial markers.

The decomposition provides a structure representation that is sensitive to compact and marginally resolved features as well as to structural patterns much larger than the FWHM of the instrumental PSF in the image.

## 2.2 Multiscale Cross-Correlation

To detect structural differences between two images of an astronomical object made at epochs  $t_1$  and  $t_2$ , one needs to find an optimal set of displacements of the original SSP (described by the groups of SSP  $S_{j,1}, j = 1, \dots, J$ ) that would match the SSP in the second image (described by  $S_{j,2}, j = 1, \dots, J$ ). Cross-correlating  $S_{j,1}$  and  $S_{j,2}$  is a well-suited tool for this purpose. There are two specific issues that need to be addressed, however, to ensure that the cross-correlation analysis is reliable. First, a viable rule needs to be introduced to identify the relevant image area across which the cross-correlation is to be applied. Second, the probability of false matching needs to be minimized for features with sizes smaller than the typical displacement between the two epochs.

These two requirements can be met by multiscale cross-correlation (MCC), which combines the structural and positional information contained in  $S_j$  at all scales of the wavelet decomposition:

1. The largest scale  $J$  of a wavelet decomposition is chosen such that the largest expected displacement is smaller than  $2^J$ .
2. Displacements of SSP features are determined at the largest scale  $J$ . For this calculation, all  $\Delta_{j,a}^{J+1}$  are set to zero, and  $\Delta_{J,a} = \delta_{J,a}$  is calculated for each SSP.
3. At each subsequent scale  $j$  ( $j < J$ ),  $\Delta_{j,a}^{j+1}$  is determined first by adopting the displacement  $\Delta_{j,a}$  measured at the  $j+1$  scale for the SSP in which the given  $j$ -scale region  $s_{j,a}$  falls. Then the total displacement for this SSP is given by  $\Delta_{j,a} = \Delta_{j,a}^{j+1} + \delta_{j,a}$ .

In this algorithm, the only quantity that needs to be calculated at each scale is the relative displacement  $\delta_{j,a}$ . This quantity can be determined reliably from the cross-correlation.

## 3. Applications to astronomical images

We have tested the performance of WISE on astronomical images by applying it to several image sequences obtained as part of the MOJAVE long-term monitoring program of extragalactic jets with very long baseline interferometry (VLBI) observations [7, and references therein] and in the M 87 “movie” project [8].

The analysis of the jet in 3C 273 was performed on 69 images, with the observations covering the time range from 1996 to 2010 and providing, on average, one observation every three months. The core separations of individual SSP obtained from WISE decomposition are compared in Fig. 1) with the results from the MOJAVE kinematic analysis based on the Gaussian model fitting of the jet structure. Comparison indicates that WISE detects consistently nearly all the components identified

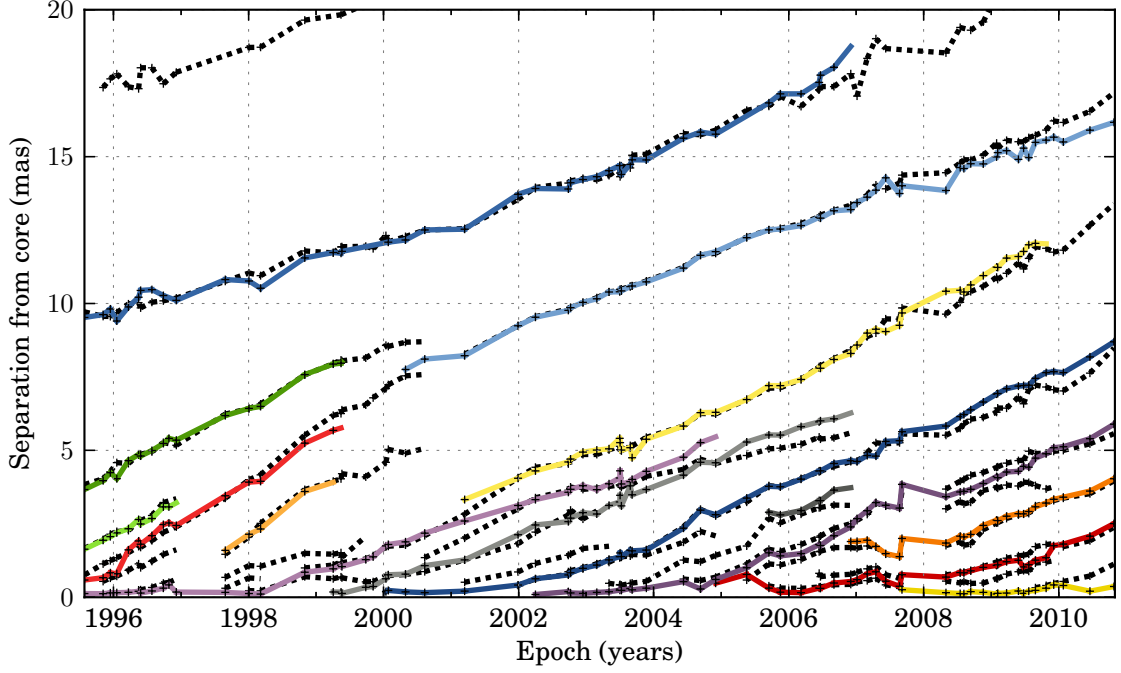


**Figure 1:** Core separation plot of the most prominent features in the jet of 3C 273 (taken from [5]). The model-fit based MOJAVE results (dashed lines) are compared with the WISE results (solid lines).

by the MOJAVE model fitting analysis, with a very good agreement on their positional locations and separation speeds.

Similar analysis was performed on 87 observations of the jet in 3C 120 between 1996 and 2010. A total of 30 moving SSP was detected. The resulting core separations of the SSP plotted in Fig. 2 generally agree very well with the separations of the jet components identified in the MOJAVE Gaussian model fit analysis.

The jet in M 87 is probably one of the most investigated. Its proximity ( $D = 16.7$  Mpc; [9]) combined with a large mass of the central black hole ( $M_{BH} \simeq 6.1 \times 10^9 M_{\odot}$ ; [10]) make it one of the primary source to probe the jet formation and acceleration at its base. We analyzed eleven epochs of the M 87 jet observed with the Very Large Baseline Array (VLBA) between 27 January 2007 and 26 August 2007 with an average of 21 days interval [8]. The velocity field obtained from WISE analysis is plotted in Fig.3. It reveals complex kinematic with subluminal and superluminal motion measured in three regions of the jet: a southern and northern sheath and a central spine.

A Stacked Normalized Cross Correlation analysis combining all SSPs obtained at all eleven epochs was performed. Result indicates the presence of 2 main speed component in all three regions of the jet. A slow mildly relativistic speed ( $\sim 0.5$  c), and a faster relativistic speed ( $\sim 2.25$  c). This could be explained by the presence of a disk wind around the jet from which only a small fraction of it at the interface could be observable through synchrotron radiation [11].

Additionally we found that the average velocity measured in the southern sheath was consistently faster than the average velocity measured in the northern sheath, suggesting jet or pattern rotation.

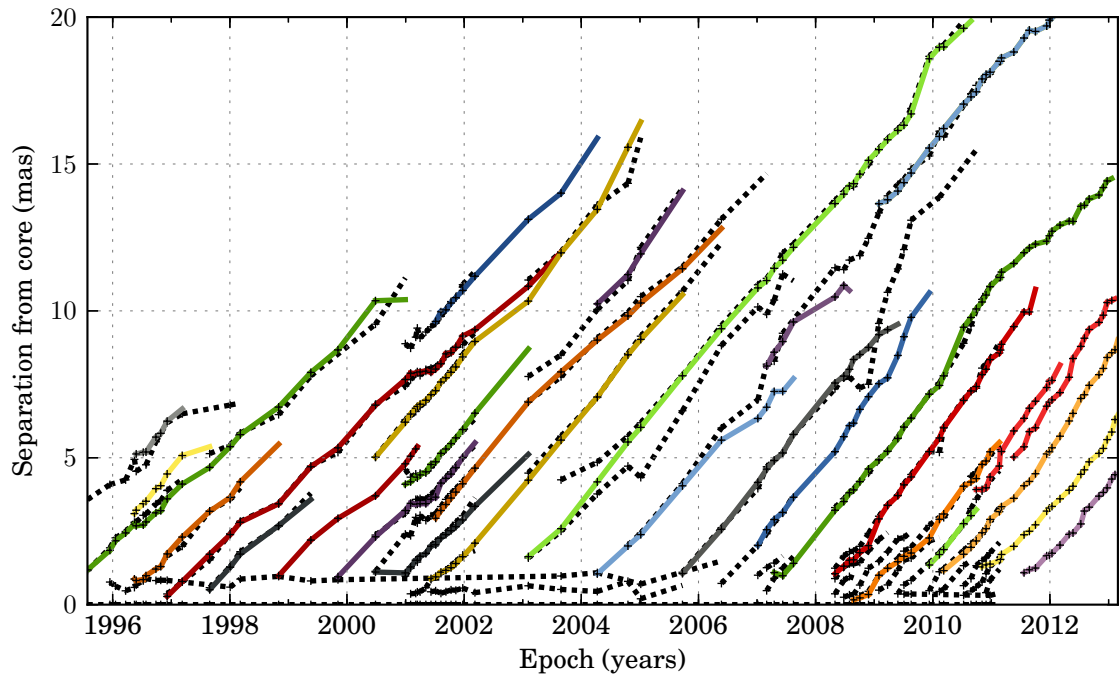


**Figure 2:** Core-separation plot of the features identified in the jet of 3C 120 (taken from [5]). The model-fit based MOJAVE results (dashed lines) are compared with the WISE results (solid lines).

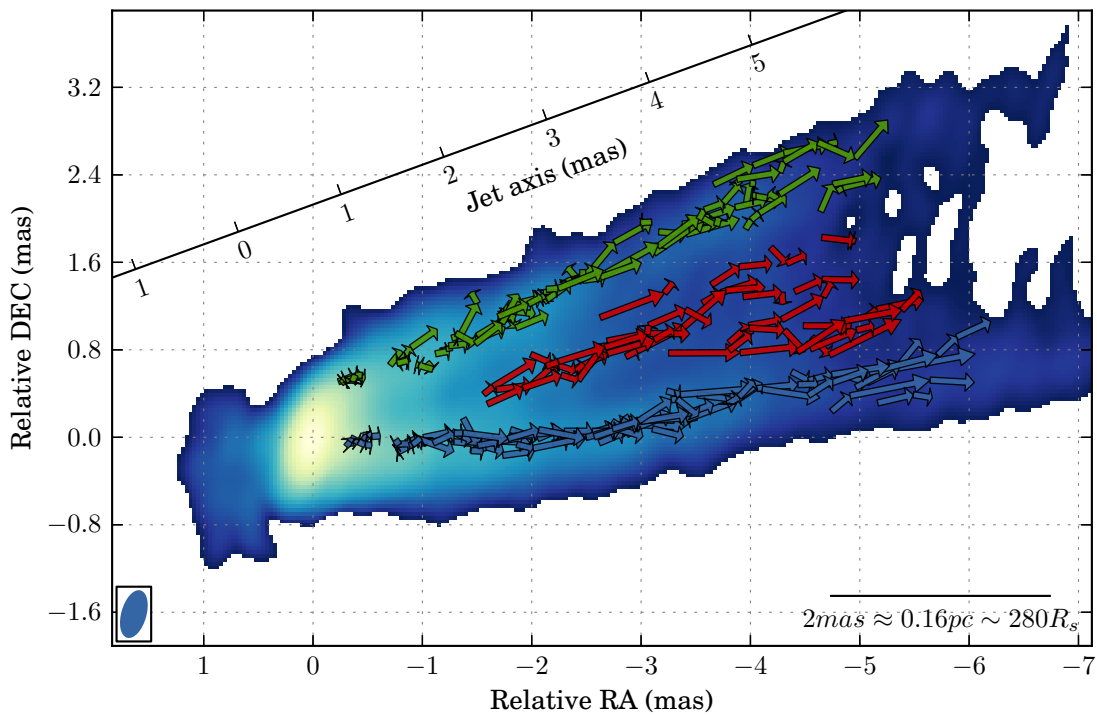


**Figure 3:** Velocity field in the jet of M 87. Three main regions are detected: a southern (blue) and northern (green) sheath and a central spine (red). Arrows represents displacement of individual SSPs between two subsequent epochs.

#### 4. Conclusions

The WISE method we presented here offers an effective and objective way to classify structural patterns in images of astronomical objects and track their evolution traced by multiple observations of the same object. The method combines automatic segmented wavelet decomposition with a multiscale cross-correlation algorithm, which enables reliable identification and tracking of statistically significant structural patterns.

We performed the analysis of several transversely resolved AGN jets observed as part of the MOJAVE project using this method. For all these sources, global kinematic changes obtained using our SWD technique were in excellent agreement with the one obtained by the MOJAVE team using model-fitting technique, demonstrating the reliability of our method for the reconstruction of the velocity field in transversely resolved flows.

Preliminary results of the application of WISE on the jets of M 87 suggests a layered jet with a fast spine surrounded by a subrelativistic disk wind. Ongoing analysis will concentrate on attempting to model velocity in combination with the collimation profile, provide an hint on the potential jet rotation, and investigate the velocities obtained in the counter jet side.

#### References

- [1] Zitová, B. & Flusser, J., *Image registration methods: a survey*, Image and Vision Computing, **21**, 977, 2003
- [2] A. P. Lobanov, *Ultracompact jets in active galactic nuclei*, A&A **330** 79, 1998.
- [3] A. P. Lobanov and J. A. Zensus, *A Cosmic Double Helix in the Archetypical Quasar 3C273*, *Science* **294** 128, 2001.
- [4] J.-L. Starck and F. Murtagh, *Astronomical image and data analysis*. Springer, 2006.
- [5] F. Mertens and A. Lobanov, *Wavelet-based decomposition and analysis of structural patterns in astronomical images*, A&A, in press, DOI: 10.1051/0004-6361/201424566 .
- [6] S. G. Mallat, *A theory for multiresolution signal decomposition - the wavelet representation*, *IEEE Transactions on Pattern Analysis and Machine Intelligence* **11** 674, 1989.
- [7] M. L. Lister, M. F. Aller, H. D. Aller et al., *Mojave. X. parsec-scale jet orientation variations and superluminal motion in active galactic nuclei*, AJ **146** 1200, 2013.
- [8] R. C. Walker, C. Ly, W. Junor et al., *A VLBA movie of the jet launch region in m87*, *Journal of Physics: Conference Series* **131** (2008), no. 1 012053.
- [9] A. Jordán, P. Côté, J. P. Blakeslee et al., *The acs virgo cluster survey. x.*, ApJ **634** 1002, 2005.
- [10] K. Gebhardt, J. Adams, D. Richstone et al., *The black-hole mass in m87 from gemini/nifs adaptive optics observations*, ApJ **729** 119, 2011.
- [11] J. Gracia, N. Vlahakis, I. Agudo et al., *Synthetic synchrotron emission maps from mhd models for the jet of m87*, ApJ **695** 503, (2009).